2024-03-11

A Mathematical Model for Transmission of Taeniasis and Neurocysticercosis

Rwabona, Gideon

Hindawi

Hindawi
Computational and Mathematical Methods
Volume 2024, Article ID 2550598, 14 pages
https://doi.org/10.1155/2024/2550598

Research Article

A Mathematical Model for Transmission of Taeniasis and Neurocysticercosis

Gideon Eustace Rwabona,[1,2] **Verdiana Grace Masanja**,[1] **Sayoki Mfinanga**,[3] **Abdoelnaser Degoot**,[4] **and Silas Mirau**[1]

[1]*School of Computation and Communication Science and Engineering, The Nelson Mandela African Institution of Science and Technology (NM-AIST), Arusha, Tanzania*
[2]*Department of Mathematics and Statistics, Mbeya University of Science and Technology, Mbeya, Tanzania*
[3]*National Institute of Medical Research, Dar es Salaam, Tanzania*
[4]*African Institute for Mathematical Sciences (AIMS) Rwanda, Kigali, Rwanda*

Correspondence should be addressed to Gideon Eustace Rwabona; rwabonag@nm-aist.ac.tz

Received 17 January 2024; Revised 12 February 2024; Accepted 22 February 2024; Published 11 March 2024

Academic Editor: Jan Rychtar

In this study, we present a mathematical model for the codynamics of taeniasis and neurocysticercosis and rigorously analyze it. To understand the underlying dynamics of the proposed model, basic system properties such as the positivity and boundedness of solutions are investigated through the completing differential process. The basic reproduction number was calculated using the next-generation matrix method, and the analysis showed that when $\mathscr{R}_0 < 1$, the disease in the community eventually dies out, and when $\mathscr{R}_0 > 1$, the diseases persist. Local stability of the equilibria was analyzed using the Jacobian matrix, and Lyapunov function techniques were used to determine the global analysis, which showed that the endemic equilibrium point was globally stable when $\mathscr{R}_0 > 1$. On the other hand, the disease-free equilibrium was determined to be globally stable when $\mathscr{R}_0 < 1$. To identify the most influential parameters of the proposed model, partial correlation coefficient techniques were used. The numerical results depict that the model aligns well with the transmission dynamics, which goes through two populations: humans and pigs, whereby the model system stabilizes after some time, showing the validity of the proposed model. Furthermore, the simulations of the proposed model revealed that the shedding habit of infected humans with taeniasis and the bad cooking habit or eating of raw or undercooked pork products have a higher impact on the spread of neurocysticercosis and taeniasis in the community. Hence, this study proposes that in order to control taeniasis and neurocysticercosis, effective disease control measures should primarily prioritize hygienic behaviour and proper cooking of pork meat to the required temperature.

1. Introduction

Neurocysticercosis (NCC) is a serious public health problem in *Taenia solium* endemic areas and in some immigrants and international travelers [1]. NCC disease is caused by a parasitic pork tapeworm at the larvae stage, called *Taenia solium* [2], that invades the central nervous system of the human brain [3]. There are two hosts for the life cycle of *Taenia solium*: humans as definitive hosts and pigs as intermediate hosts for reproduction. Pigs acquire the infection when they ingest human faeces containing *Taenia solium* eggs and subsequently evolve into cysticerci or cysts [4]. When people consume raw or undercooked pork product containing cysticerci, they can develop an intestinal tapeworm infection at the stage of adult tapeworm called taeniasis, but not NCC [5]. Humans can also become intermediate hosts by directly ingesting *Taenia solium* eggs from their surrounding environment. These eggs then evolve into cysticerci that migrate mostly into the central nervous system causing NCC. Some NCC cases can result in epilepsy [6]. The main source of *Taenia solium* eggs is humans infected with taeniasis who excrete faeces in an environment where

pigs and other humans can easily access them and get infected. In this scenario, there is a possibility of autoinfection, causing a high risk of developing NCC for people who are infected with taeniasis [7].

The World Health Organization (WHO) considers NCC as one of the most neglected tropical diseases and a major cause of epilepsy in regions where pigs are free-ranging and hygiene is poor [8]. Moreover, pork production is expected to increase in the next decade in sub-Saharan Africa [9]; hence, NCC will likely become more prevalent [10]. Despite the efforts to eliminate taeniasis and NCC, the diseases are still endemic and persisting in many pig-raising regions around the globe, especially in sub-Saharan Africa, Southeast Asia, and Latin America [11]. Its burden has accounted for an estimated 2.8 million disability-adjusted life years lost globally [12, 13].

The burden of taeniasis and NCC in Africa is not well-documented due to limited surveillance systems and underreporting. However, several studies have highlighted their significant prevalence in certain regions. A study in Cameroon reported NCC prevalence to be 29% among patients with epilepsy [14]. Taeniasis and NCC are both common in Tanzania, with high prevalence rates reported in various regions of the country [15]. A study conducted in rural areas of Tanzania found a high prevalence of taeniasis, with up to 20% of the population infected [16]. According to [17], the prevalence of taeniasis was found to be 21.4% in a sample of 300 schoolchildren in Dar es Salaam, while another study published in [15] reported a prevalence of 14.1% in a sample of 200 patients with abdominal pain in Dar es Salaam. NCC is a significant public health concern in Tanzania, with a prevalence rate of 2.3% reported in [15, 18]. This prevalence rate is higher than the global average, which is estimated to be around 1% [19]. Other studies from rural Northern Tanzania reported that the estimates of the prevalence of NCC among people with epilepsy range from 4 to 18%, but the overall estimates go even up to 30% in people with epilepsy in endemic areas [16]. The association between NCC and epilepsy can reach 70% [17, 18].

The insights from mathematical modeling have been used intensively to study the dynamics of infectious diseases for decades. Recently, authors modelled the Middle East respiratory syndrome coronavirus (MERS-CoV) with different approaches, both aligning with mathematical modeling. For instance, [20] modelled the epidemic trend of MERS-CoV with optimal control using a deterministic theoretical model to understand the transmission between individuals and MERS-CoV reservoirs such as camels. Also, MERS-CoV has been studied using fractional operators with the next-generation matrix method [21]. Other mathematical models that have been devoted to studying this emerging disease can be found in [22, 23] and [24].

The dynamics and control of parasite foodborne infections have been studied through the years using a variety of mathematical models [25–27]. These models can aid in understanding infectious disease dynamics and determine the most effective prevention strategies. Despite the number of studies devoted to modeling the transmission dynamics of taeniasis and cysticercosis [5, 28–31], little attention is given to the dynamics of NCC. Additionally, the codynamics, which is a result of the complex life cycle of the *Taenia solium* worm, has not been given preferable consideration. Motivated by the above-cited mathematical models, and for the purpose of better understanding the transmission dynamics of taeniasis and NCC, the study proposes a mathematical model for taeniasis and NCC codynamics transmission with autoinfection and coinfection.

The novelty of our work is that we studied the transmission dynamics of taeniasis, NCC codynamics, and autoinfection using a mathematical modeling approach, as none of the studies in the literature have studied the complex dynamic behaviour of the model.

This work is organized as follows: Section 2 presents taeniasis and NCC codynamic transmission model formulation. Section 3 presents a model analysis. In Section 4, it shows the numerical results and discussion, while Section 5 discusses the conclusion.

2. Model Formulation

The proposed model considers the human population $N_h(t)$, the pig population $N_p(t)$, the *Taenia solium* eggs in the environment $E(t)$, and the concentration of cysts in the infected pork products $P(t)$. This model is inspired by the work of [31, 32] and formulated by adding the infected pork meat to account for the concentration of cysts compartment and NCC compartment to account for humans with NCC and/or taeniasis. The model is governed by the following assumptions with notations therein.

The human population $N_h(t)$ is divided into three classes, namely, susceptible $S_h(t)$, infected with taeniasis $I_T(t)$, and infected with NCC $I_N(t)$. The pig population is also divided into susceptible pigs $S_p(t)$ and infected pigs $I_p(t)$. The total populations, for humans and pigs at any time are, respectively, given by $N_h(t) = S_h(t) + I_T(t) + I_N(t)$ and $N_p(t) = S_p(t) + I_p(t)$.

Each human class incurs a natural death at the rate of μ_h. Susceptible are subject to increase by a constant recruitment rate of Λ_h through birth and move to class I_T at rate β_T and to class I_N at rate β_N. The transmission of both the cysts from infected pork and *Taenia solium* eggs from the environment to human that results in NCC is assumed to be density dependent. Thus, the force of infection at which individuals acquire taeniasis is defined as

$$\lambda_T = \beta_T P(t) S_h(t), \tag{1}$$

where β_T is the effective transmission rate of cysts upon consumption of infected pork meat. The force of infection at which S_h and I_T acquire NCC, respectively, is defined as

$$\begin{aligned} \lambda_N &= \beta_N E(t) S_h(t), \\ \lambda_B &= \beta_B E(t) I_T(t), \end{aligned} \tag{2}$$

where β_N and β_B are the effective contact rates between human and *Taenia solium* eggs in a contaminated environment.

The number of susceptible pigs increases by birth at the rate of Λ_p, become infected with cysts due to digesting *Taenia solium* eggs in the environment at the rate of β_p, and die naturally at the rate of μ_p. Infected pigs are slaughtered at the rate of ω. Natural recovery for cysts-infected pigs takes a long time [31], and therefore, we assumed no natural recovery. The transmission rate of *Taenia solium* eggs to the pig is modelled as the product of the contact rate and the probability of infection upon feeding on *Taenia solium* eggs from the environment. The force of infection by which pigs acquire infection is defined as

$$\lambda_p = \beta_P E(t) S_p(t), \tag{3}$$

where β_P is the effective contact rate between pig and *Taenia solium* eggs in a contaminated environment.

The number of eggs consumed by pigs and humans has a negligible effect on the total number of eggs present in the environment because of the plethora of eggs in the environment while it can take a few eggs to cause the infection [31]. *Taenia solium* eggs contaminate$E(t)$at a rate ofσ, and as a result of humans infected with taeniasis defecating in the environment and diminish naturally at the rate ofα,$P(t)$ increases at the rate ofωas result of slaughtering infected pigs and removed naturally or otherwise by the rate ofδ.

In light of the aforementioned assumptions, the dynamics of the proposed model are shown in Figure 1 and captured by the following set of ordinary differential equations:

$$\left.\begin{aligned}
S_h'(t) &= \Lambda_h - (\beta_T P(t) + \beta_N E(t) + \mu_h) S_h(t),\\
I_T'(t) &= \beta_T P(t) S_h(t) - (\beta_B E(t) + \mu_h) I_T(t),\\
I_N'(t) &= \beta_N E(t) S_h(t) + \beta_B E(t) I_T(t) - (\mu_h + \mu_N) I_N(t),\\
S_P'(t) &= \Lambda_P - \left(\beta_p E(t) + \mu_p\right) S_p(t),\\
I_p'(t) &= \beta_P E(t) S_p(t) - \left(\mu_p + \omega\right) I_p(t),\\
P'(t) &= \omega I_p(t) - \delta P(t),\\
E'(t) &= \sigma I_T(t) - \alpha E(t),
\end{aligned}\right\} \tag{4}$$

with the following initial conditions

$$\begin{aligned}
S_h(0) &= S_{h0} \geq 0,\\
I_T(0) &= I_{T0} \geq 0,\\
I_N(0) &= I_{N0} \geq 0,\\
S_p(0) &= S_{p0} \geq 0,\\
I_p(0) &= I_{p0} \geq 0,\\
P(0) &= P_0 \geq 0,\\
E(0) &= E_0 \geq 0.
\end{aligned} \tag{5}$$

3. Analysis of the Model

This section presents the boundedness and model positivity as well as the computation of the basic reproduction number of model (4) and the stability of disease-free and endemic equilibrium.

3.1. Positivity of Model Solutions. In this section, we prove the positivity of the proposed model solutions by proving Theorem 1.

Theorem 1. *Let the initial condition of model (4) be nonnegative, then the solution* $(S_h, I_T, I_N, S_p, I_p, P, E)$ *is positive for all* $t > 0$.

Proof. Consider the first equation in model (4), which is

$$S_h'(t) = \Lambda_h - (\beta_T P(t) + \beta_N E(t) + \mu_h) S_h(t). \tag{6}$$

If we ignore the positive terms, Equation (6) becomes

$$\frac{dS_h}{dt} \geq -(\beta_T P(t) + \beta_N E(t) + \mu_h) S_h(t). \tag{7}$$

By separating the variables in Equation (7) and integrating them, we have

$$S_h \geq C e^{-\int_0^t (\beta_T P(t) + \beta_N E(t) + \mu_h) ds}. \tag{8}$$

Applying the initial condition, we obtain

$$S_h(t) \geq S_h(0) e^{-\int_0^t (\beta_T P(t) + \beta_N E(t) + \mu_h) ds} \geq 0. \tag{9}$$

By the same approach, we establish that

$$\begin{aligned}
I_T(t) &\geq I_t(0) e^{-\int_0^t (\mu_h + \beta_B E(s)) ds} \geq 0,\\
I_N(t) &\geq I_N(0) e^{-(\mu_h + \mu_N) t} \geq 0,\\
S_p(t) &\geq S_p(0) e^{-\int_0^t \left(\beta_p E(s) + \mu_p\right) ds} \geq 0,\\
I_p(t) &\geq I_p(0) e^{-\left(\mu_p + \omega\right) t} \geq 0,\\
P(t) &\geq P(0) e^{-\delta t} \geq 0,
\end{aligned} \tag{10}$$

$$E(t) \geq E(0) e^{-\alpha t} \geq 0. \tag{11}$$

Therefore, we can conclude that the proposed model is positive for all $t > 0$. □

3.2. Bounded Region. The invariant region serves to show the feasibility of the model solutions. Recall that $N_h(t) = S_h(t) + I_T(t) + I_N(t)$ and $N_p(t) = S_p(t) + I_p(t)$ for human and pig populations, respectively. Starting with the human population, we have

$$N_h'(t) = S_h'(t) + I_T'(t) + I_N'(t). \tag{12}$$

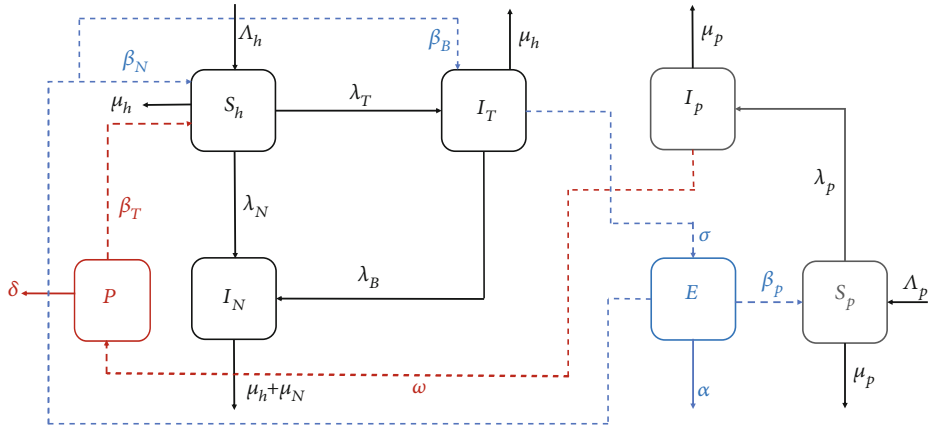

Figure 1: Flow diagram for the transmission dynamics of taeniasis and NCC codynamics model (4), where λ_T is given in Equation (1), λ_N and λ_B are given in Equation (2), and λ_P is given in Equation (3).

Substituting the derivatives from model (4) into Equation (12) and upon simplification, we get

$$N_h'(t) = \Lambda_h - \mu_h N_h(t) - \mu_N I_N. \tag{13}$$

From Equation (13) it can be observed that

$$\frac{dN_h}{dt} \leq \Lambda_h - \mu_h N_h. \tag{14}$$

By solving Equation (14) and applying the initial conditions of the model (4), we obtain

$$N_h(t) \leq \frac{\Lambda_h}{\mu_h} + \left(N_h(0) - \frac{\Lambda_h}{\mu_h}\right)e^{-\mu_h t}. \tag{15}$$

As $t \longrightarrow \infty$, Equation (15) reduces to $N_h(0) \leq \Lambda_h/\mu_h$. Since human population is nonnegative, implies that $0 \leq N_h(t) \leq \Lambda_h/\mu_h$

When the same procedure is applied to the pig population as $t \longrightarrow \infty$, we obtain

$$0 \leq N_p(t) \leq \frac{\Lambda_p}{\mu_p}. \tag{16}$$

Since $N_h(t) \leq \Lambda_h/\mu_h$ and $N_p(t) \leq \Lambda_p/\mu_p$, then $I_T(t) \leq \Lambda_h/\mu_h$, $I_N(t) \leq \Lambda_h/\mu_h$, and $I_p(t) \leq \Lambda_p/\mu_p$. It follows the same for the concentration of *Taenia solium* eggs in the environment and cysts concentration in the infected pork products, when $t \longrightarrow \infty$, we have, respectively

$$\begin{aligned} P(t) &\leq \frac{\Lambda_p}{\mu_p}\frac{\omega}{\delta}, \\ E(t) &\leq \frac{\Lambda_h}{\mu_h}\frac{\sigma}{\alpha}. \end{aligned} \tag{17}$$

Therefore, the proposed model (4) is a positive variant in the region

$$\begin{aligned} \Sigma = \Bigg\{ \left(S_h, I_T, I_N, S_p, I_p, P, E\right) \in \mathbb{R}_+^7 \Bigg| N_h(t) \leq \frac{\Lambda_h}{\mu_h}, N_p(t) \\ \leq \frac{\Lambda_p}{\mu_p}, P(t) \leq \frac{\Lambda_p}{\mu_p}\frac{\omega}{\delta}, E(t) \leq \frac{\Lambda_h}{\mu_h}\frac{\sigma}{\alpha} \Bigg\}. \end{aligned} \tag{18}$$

Hence, the proposed model (4) has biological and epidemiological meaning.

3.3. Disease-Free Equilibrium. The disease-free equilibrium (DFE) of model (4) is obtained by setting the right-hand sides of the equations of model (4) to zero, and it is given by

$$E_0 = \left(\frac{\Lambda_h}{\mu_h}, 0, 0, \frac{\Lambda_p}{\mu_p}, 0, 0, 0\right). \tag{19}$$

In other words, the DFE occurs in the absence of both taeniasis and NCC in humans and when there are no infections in pigs.

3.4. Basic Reproduction Number. The basic reproduction number $\mathcal{R}_0$ is an important quantity in epidemiology that measures the potential for disease transmission within a population. $\mathcal{R}_0$ represents the average number of secondary infections that can be generated by a single infected individual in a susceptible population and quantifies the transmissibility of a disease [33]. When $\mathcal{R}_0 < 1$, the disease dies out in the population, and when $\mathcal{R}_0 > 1$, the disease remains persistent [34]. We computed $\mathcal{R}_0$ for model (4) using the approach described in [33–35].

To apply the technique in [34], we rewrite the model system (4) as

$$\frac{dx}{dt} = \mathcal{F}(x) - \mathcal{V}(x), \tag{20}$$

with $\mathcal{V}_i = \mathcal{V}_i^- - \mathcal{V}_i^+$.

As pointed out in [34], $\mathscr{R}_0$ is given by the spectral radius of the next-generation matrix defined as

$$G = FV^{-1} = \left[\frac{\partial \mathscr{F}_i}{\partial X_j}(E_o)\right]\left[\frac{\partial \mathscr{F}_i}{\partial X_j}(E_o)\right]^{-1}, \tag{21}$$

where $\mathscr{F}_i$ denotes new infectious and $\mathscr{V}_i$ transfer terms with $i, j = 1, 2, 3, 4, 5$ for the infected classes of model (4). Then, $\mathscr{F}_i$, $\mathscr{V}_i^-$, and $\mathscr{V}_i^+$ are obtained from the infected classes of model (4) which are I_T, I_N, I_p, P and E and given in Equation (22).

$$\mathscr{F}(x) = \begin{pmatrix} \beta_T P S_h \\ \beta_N E S_h \\ \beta_p E S_p \\ 0 \\ 0 \end{pmatrix},$$

$$\mathscr{V}^+(x) = \begin{pmatrix} 0 \\ \beta_B I_T \\ 0 \\ \omega I_p \\ \sigma I_T \end{pmatrix}, \tag{22}$$

$$\mathscr{V}^-(x) = \begin{pmatrix} (\beta_N E + \mu_h) I_T \\ (\mu_h + \mu_N) I_N \\ \left(\mu_p + \omega\right) I_p \\ \delta P \\ \alpha E \end{pmatrix}.$$

The elements in vectors $\mathscr{F}_i$ and $\mathscr{V}_i$ are expressed as the derivatives with respect to the infected states, and their associated Jacobian matrices evaluated at E_0 are given by

$$\boldsymbol{F} = \begin{pmatrix} 0 & 0 & 0 & \dfrac{\beta_T \Lambda_h}{\mu_h} & 0 \\ 0 & 0 & 0 & 0 & \dfrac{\beta_N \Lambda_h}{\mu_h} \\ 0 & 0 & 0 & 0 & \dfrac{\beta_P \Lambda_p}{\mu_p} \\ 0 & 0 & 0 & 0 & 0 \\ 0 & 0 & 0 & 0 & 0 \end{pmatrix},$$

$$\boldsymbol{V} = \begin{pmatrix} \mu_h & 0 & 0 & 0 & 0 \\ 0 & \mu_h + \mu_N & 0 & 0 & 0 \\ 0 & 0 & \left(\mu_p + \omega\right) & 0 & 0 \\ 0 & 0 & -\omega & \delta & 0 \\ -\sigma & 0 & 0 & 0 & \alpha \end{pmatrix}, \tag{23}$$

$$V^{-1} = \begin{pmatrix} \dfrac{1}{\mu_h} & 0 & 0 & 0 & 0 \\ 0 & \dfrac{1}{\mu_h + \mu_N} & 0 & 0 & 0 \\ 0 & 0 & \dfrac{1}{\mu_p + \omega} & 0 & 0 \\ 0 & 0 & \dfrac{\omega}{\delta}\dfrac{1}{\left(\mu_p + \omega\right)} & \dfrac{1}{\delta} & 0 \\ \dfrac{\sigma}{\alpha}\dfrac{1}{\mu_h} & 0 & 0 & 0 & \dfrac{1}{\alpha} \end{pmatrix}. \tag{24}$$

Using matrix F in Equation (23) and matrix V^{-1} in (24), matrix G in (25) is obtained.

$$G = \begin{pmatrix} 0 & 0 & \dfrac{\Lambda_h \beta_T \omega}{\delta \mu_h \left(\mu_p + \omega\right)} & \dfrac{\Lambda_h \beta_T}{\delta \mu_h} & 0 \\ \dfrac{\Lambda_h \beta_N \sigma}{\alpha \mu_h^2} & 0 & 0 & 0 & \dfrac{\Lambda_h \beta_N}{\alpha \mu_h} \\ \dfrac{\Lambda_p \beta_p \sigma}{\alpha \mu_h \mu_p} & 0 & 0 & 0 & \dfrac{\Lambda_p \beta_p}{\alpha \mu_p} \\ 0 & 0 & 0 & 0 & 0 \\ 0 & 0 & 0 & 0 & 0 \end{pmatrix}. \tag{25}$$

Eigenvalues of G are

$$\left\{ -\sqrt{\frac{\Lambda_h \Lambda_p \beta_T \beta_p \omega \sigma}{\alpha \delta \mu_p \mu_h^2 \left(\mu_p + \omega\right)}}, \sqrt{\frac{\Lambda_h \Lambda_p \beta_T \beta_p \omega \sigma}{\alpha \delta \mu_p \mu_h^2 \left(\mu_p + \omega\right)}}, 0, 0, 0 \right\}. \tag{26}$$

Therefore, the basic reproduction number was found to be

$$\mathscr{R}_0 = \sqrt{\frac{\Lambda_h \Lambda_p \beta_T \beta_p \omega \sigma}{\alpha \delta \mu_p \mu_h^2 \left(\mu_p + \omega\right)}}. \tag{27}$$

The basic reproduction number consists of two terms which characterize the contribution from the different pathways (human and pig populations) to new infections. For better biological interpretation, Equation (27) can be rearranged as

$$\mathscr{R}_0 = \sqrt{\mathscr{R}_{0h} . \mathscr{R}_{0p}}, \tag{28}$$

where

$$\mathscr{R}_{0h} = \frac{\Lambda_h \beta_T \sigma}{\alpha \mu_h^2}, \tag{29}$$

$$\mathscr{R}_{0p} = \frac{\Lambda_p \beta_p \omega}{\delta \mu_p \left(\mu_p + \omega\right)}. \tag{30}$$

Equations (29) and (30) propose the partial basic reproduction number for the human population and pig population as

the subbasic reproduction numbers for the whole model system (4). Here, $\mathscr{R}_{0h}$ describes the number of humans that one infectious pig infects over its expected infection period in a completely susceptible human population, and $\mathscr{R}_{0h}$ describes the number of pigs infected by one infectious human during the period of infectiousness in a completely susceptible pig population.

In Equation (27), $1/\mu_h$ is the life expectancy for human, $1/\mu_p + \omega$ is the average life time cysts-infected pig, Λ_h/μ_h and Λ_p/μ_p are, respectively, the initial populations for susceptible humans and pigs, and ω/δ and σ/α are, respectively, the density of *Taenia solium* larvae cysts in the contaminated pork meat and *Taenia solium* eggs released by humans with taeniasis.

3.5. Local Stability of Disease-Free Equilibrium. The dynamical system of model (4) is nonlinear. Its local stability is determined from the sign of the eigenvalues of the corresponding Jacobian matrix at the disease-free equilibrium point (E_0). The Jacobian matrix at E_0 is given by

$$J(E_0) = \begin{pmatrix} -\mu_h & 0 & 0 & 0 & 0 & \frac{\Lambda_h\beta_T}{\mu_h} & \frac{\Lambda_h\beta_N}{\mu_h} \\ 0 & -\mu_h & 0 & 0 & 0 & \frac{\Lambda_h\beta_T}{\mu_h} & 0 \\ 0 & 0 & -(\mu_h+\mu_N) & 0 & 0 & 0 & \frac{\Lambda_h\beta_N}{\mu_h} \\ 0 & 0 & 0 & -\mu_p & 0 & 0 & 0 \\ 0 & 0 & 0 & 0 & -(\mu_p+\omega) & 0 & \frac{\Lambda_p\beta_p}{\mu_p} \\ 0 & 0 & 0 & 0 & \omega & -\delta & 0 \\ 0 & \sigma & 0 & 0 & 0 & 0 & -\alpha \end{pmatrix}. \tag{31}$$

Theorem 2. *The disease-free equilibrium is locally asymptotically stable if $\mathscr{R}_0 < 1$, and all eigenvalues of the Jacobian matrix at E_0 have negative real parts, and if $\mathscr{R}_0 > 1$, E_0 is unstable.*

Proof. The first, third, and fourth columns of the matrix $J(E_0)$ in Equation (31) contain only the diagonal terms, which gives the first three eigenvalues: $\lambda_1 = \mu_h$, $\lambda_2 = -(\mu_h + \mu_N)$, and $\lambda_3 = -\mu_p$. Thus, the matrix $J(E_0)$ reduces to

$$J'(E_0) = \begin{pmatrix} -\mu_h & 0 & \frac{\Lambda_h\beta_T}{\mu_h} & 0 \\ 0 & -(\mu_p+\omega) & 0 & \frac{\Lambda_p\beta_p}{\mu_p} \\ 0 & \omega & -\delta & 0 \\ \sigma & 0 & 0 & -\alpha \end{pmatrix}. \tag{32}$$

From Equation (32), the characteristic polynomial of matrix $J'(E_0)$ is given by

$$\lambda^4 + a_1\lambda^3 + a_2\lambda^2 + a_3\lambda + a_4 = 0, \tag{33}$$

where

$$\left.\begin{aligned} a_1 &= (\mu_h+\alpha)\delta + \mu_p + \omega + \delta > 0, \\ a_2 &= ((\mu_h+\alpha)\delta + \delta)(\mu_p+\omega) + \mu_h\alpha + (\mu_h+\alpha)\delta > 0, \\ a_3 &= \mu_h\alpha\delta + \mu_h + (\mu_h+\alpha)\delta > 0, \\ a_4 &= \frac{\Lambda_h\Lambda_p\beta_T\beta_p\sigma\omega}{\mu_h\mu_p} + \mu_h\alpha\delta(\mu_p+\omega) > 0. \end{aligned}\right\} \tag{34}$$

Note that λ represents the eigenvalues and $a_i (i = 1, 2, 3, 4)$ are the coefficients of the characteristic polynomial. It is evidently seen that all coefficients of the characteristics polynomial in Equation (33) are positive; by applying the Routh-Hurwitz criterion, the other four eigenvalues of the matrix in Equation (32) will also have negative real parts.

Since all eigenvalues of the Jacobian matrix $J(E_0)$ evaluated at E_0 have negative real parts, then model system (4) is locally asymptotically stable when $\mathscr{R}_0 < 1$. □

3.6. Global Stability of Disease-Free Equilibrium. Model (4) is said to be stable if its disease-free equilibrium is upheld when the introduction of small or large perturbation (infected individuals) into the system, and it will be globally stable if the disease persists no more, regardless of the size of the perturbation that has been introduced. In this section, we determine the global stability of model (4) at E_0 using the approach described in [36, 37].

Theorem 3. *The disease-free equilibrium of model (4) is globally asymptotically stable in the invariant region Σ, if and only if $\mathscr{R}_0 < 1$, and unstable otherwise.*

Proof. Let $B = [I_T, I_N, I_p, P, E]^T$ be the vector of the state variables of the infected classes in model (4), and consider the following comparison principle.

$$B' \le (\boldsymbol{F} - \boldsymbol{V})B, \tag{35}$$

where $\boldsymbol{F}$ and $\boldsymbol{V}$ are defined in Equation (23) and $B' = (I_T', I_N', I_p', P', E')^T$ is derivative of B. Note that $\boldsymbol{F}$ and $\boldsymbol{V^{-1}}$ are triangular matrices and meet the definition of the Metzler matrices. Then, by the Perron-Frobenius theorem [38], the dominant eigenvalue of $\boldsymbol{FV^{-1}}$ and $\boldsymbol{V^{-1}F}$ is equal, and there exists a nonnegative Perron-Frobenius vector $\boldsymbol{h}$ such that

$$\rho(\boldsymbol{V^{-1}F}) = \rho(\boldsymbol{FV^{-1}}) = h^T V^{-1} F. \tag{36}$$

This implies that

$$\boldsymbol{h}^T \boldsymbol{V}^{-1} \boldsymbol{F} = \mathscr{R}_0 \boldsymbol{h}^T. \tag{37}$$

Motivated by [39], consider a Lyapunov function

$$\eta(t) = \boldsymbol{h}^T \boldsymbol{V}^{-1} B. \tag{38}$$

Differentiating Equation (38) with respect to the infected states in model (4) and substituting them into Equation (35) yield

$$\begin{aligned} \eta'(t) &= \boldsymbol{h}^T \boldsymbol{V}^{-1} B' \leq \boldsymbol{h}^T \boldsymbol{V}^{-1} (\boldsymbol{F} - \boldsymbol{V}) B \\ &= (\mathscr{R}_o - 1) \boldsymbol{h}^T B \forall \boldsymbol{h}^T B \geq 0. \end{aligned} \tag{39}$$

The stability of the Lyapunov function, $\eta'(t) = (\mathscr{R}_0 - 1)\boldsymbol{h}^T B \leq 0$, can only occur when $\mathscr{R}_o \leq 0$. If $\eta'(t) = 0$, then $\boldsymbol{h}^T B = 0$ as well. Since the Perron-Frobenius eigenvector $\boldsymbol{h}$ has nonnegative entries, then vector B will result in $(I_T, I_N, I_p, P, E) = (0, 0, 0, 0, 0, 0)$; by substituting these values in model (4), disease-free equilibrium is obtained as

$$E^0 = \left(\frac{\Lambda_h}{\mu_h}, 0, 0, \frac{\Lambda_p}{\mu_p}, 0, 0, 0 \right). \tag{40}$$

When $\eta(t) = 0$, vector B converges to $(0, 0, 0, 0, 0, 0)$ as $t \longrightarrow \infty$, indicating that the transmission variables I_T, I_N, I_p, P, and E lose their transmission energy to susceptible classes, and hence the system returns to disease-free equilibrium. Therefore, every solution in the region Σ converges to a disease-free equilibrium point, E_0 as $t \longrightarrow \infty$ for $\mathscr{R}_0 < 1$. Thus, by LaSalle's invariant principle [37] E_0 is globally asymptotically stable in region Σ when $\mathscr{R}_0 < 1$. □

3.7. Endemic Equilibrium Point. The endemic equilibrium point denoted by E_1 is defined as a steady state solution for system (4), which occurs when there is persistence of the taeniasis and NCC in the population. E_1 is obtained by equating the right-hand side equal to zero of system (4) by zero and solving for S_h, I_T, I_N, S_P, I_p, P, and E, resulting into

$$E_1 = \left(S_h^*, I_T^*, I_N^*, S_P^*, I_p^*, P^*, E^* \right), \tag{41}$$

where

$$\begin{aligned}
S_h^* &= \frac{\Lambda_h \delta \left(\mu_p + \omega\right)\left(\mu_p + \beta_P E^*\right)}{\beta_T \omega \Lambda_p \beta_P E^* + \beta_N E^* \delta \left(\mu_p + \omega\right)\left(\mu_p + \beta_P E^*\right) + \mu_h \delta \left(\mu_p + \omega\right)\left(\mu_p + \beta_P E^*\right)}, \\
I_T^* &= \frac{\Lambda_h \beta_T \omega \Lambda_p \beta_P E^* \delta \left(\mu_p + \omega\right)\left(\mu_p + \beta_P E^*\right)}{(\beta_B E^* + \mu_h)\left(\beta_T \omega \Lambda_p \beta_P E^* + \beta_N E^* \delta \left(\mu_p + \omega\right)\right)\left(\mu_p + \beta_P E^* + \mu_h \delta \left(\mu_p + \omega\right)\left(\mu_p + \beta_P E^*\right)\delta \left(\mu_p + \omega\right)\left(\mu_p + \beta_P E^*\right)\right)}, \\
I_N^* &= \frac{\left(\Lambda_h \beta_N E^* (\beta_B E^* + \mu_h)\delta \left(\mu_p + \omega\right)\left(\mu_p + \beta_P E^*\right) + \beta_B E^* \Lambda_h \beta_T \omega \Lambda_p \beta_P E^*\right)\delta \left(\mu_p + \omega\right)\left(\mu_p + \beta_P E^*\right)}{(\mu_h + \mu_N)(\beta_B E^* + \mu_h)\left(\beta_T \omega \Lambda_p \beta_P E^* + \beta_N E^* \delta \left(\mu_p + \omega\right)\left(\mu_p + \beta_P E^*\right) + \mu_h \delta \left(\mu_p + \omega\right)\left(\mu_p + \beta_P E^*\right)\right)\delta \left(\mu_p + \omega\right)\left(\mu_p + \beta_P E^*\right)}, \\
S_p^* &= \frac{\Lambda_P}{\beta_P E^* + \mu_p}, I_p = \frac{\Lambda_p \beta_P E^*}{\left(\mu_p + \omega\right)\left(\mu_p + \beta_P E^*\right)}, P^* = \frac{\omega \Lambda_p \beta_P E^*}{\delta \left(\mu_p + \omega\right)\left(\mu_p + \beta_P E^*\right)}, E^* = E^*.
\end{aligned} \tag{42}$$

Note that the equilibrium point is solved in terms of E^*. When $S_h^* = I_T^* = I_N^* = I_p^* = P^* = E^* = 0$, we have a free equilibrium point. Otherwise, when $S_h^* \neq 0$, $I_T^* \neq 0$, $I_N^* \neq 0$, $I_p^* \neq 0$, $P^* \neq 0$, and $E^* \neq 0$, we have disease endemic equilibrium point E_1.

3.8. Stability Analysis of Endemic Equilibrium. In this section, we prove the global stability of endemic equilibrium E^* using a Lyapunov global asymptotic stability theorem [40, 41].

Theorem 4. *The endemic equilibrium E_1 is globally asymptotically stable if $\mathscr{R}_0 > 1$ and unstable otherwise.*

Proof. Define a positive definite function $H : \varepsilon^* \in \mathbb{R}_+^7 \longrightarrow \mathbb{R}$, for all $\varepsilon^* \in \Sigma$ to be a Lyapunov function for taeniasis and NCC dynamics, such that $H(E_1) = 0$ and $H(E_2) > 0$ for all $E_2 \in \Sigma - \{E_1\}$. Hence, we need to show that $dH(E_1)/dt = 0$ and $dH(E_2)/dt < 0$ which depicts that all solutions in Σ converge to E_1 as time goes to infinity.

Assume $H = H(S_h, I_T, I_N, S_p, I_p, P, E)$ be a candidate Lyapunov function given by

$$\begin{aligned} H = {} & S_h - S_h^* + S_h^* \ln \frac{S_h^*}{S_h} + I_T - I_T^* + I_T^* \ln \frac{I_T^*}{I_T} + I_N - I_N^* \\ & + I_N^* \ln \frac{I_N^*}{I_N} + S_p - S_p^* + S_p^* \ln \frac{S_p^*}{S_p} + I_p - I_p^* + I_p^* \ln \frac{I_p^*}{S_p} \\ & + P - P^* + P^* \ln \frac{P^*}{P} + E - E^* + E^* \ln \frac{E^*}{E}. \end{aligned} \tag{43}$$

Computing Equation (43) at taeniasis and NCC endemic equilibrium point, E_1 yields

$$H\left(S_h^*, I_T^*, I_N^*, S_p^*, I_p^*, P^*, E^*\right) = 0. \tag{44}$$

Then, we find the Hessian matrix M of H at

$$E_2 = H\left(S_h, I_T, I_N, S_p, I_p, P, E\right), \tag{45}$$

hence, this matrix is given by $M = \nabla^2 H(E_2)$. Thus,

$$M = \begin{pmatrix} \frac{S_h^*}{S_h^2} & 0 & 0 & 0 & 0 & 0 & 0 \\ 0 & \frac{I_T^*}{I_T^2} & 0 & 0 & 0 & 0 & 0 \\ 0 & 0 & \frac{I_N^*}{I_N^2} & 0 & 0 & 0 & 0 \\ 0 & 0 & 0 & \frac{S_p^*}{S_p^2} & 0 & 0 & 0 \\ 0 & 0 & 0 & 0 & \frac{I_p^*}{I_p^2} & 0 & 0 \\ 0 & 0 & 0 & 0 & 0 & \frac{P^*}{P^2} & 0 \\ 0 & 0 & 0 & 0 & 0 & 0 & \frac{E^*}{E^2} \end{pmatrix}. \tag{46}$$

Eigenvalues of matrix M are

$$\begin{aligned} & \frac{S_h^*}{S_h^2} > 0, \\ & \frac{I_T^*}{I_T^2} > 0, \\ & \frac{I_N^*}{I_N^2} > 0, \\ & \frac{S_p^*}{S_p^2} > 0, \\ & \frac{I_p^*}{I_p^2} > 0, \\ & \frac{P^*}{P^2} > 0, \\ & \frac{E^*}{E^2} > 0. \end{aligned} \tag{47}$$

Table 1: Parameter values of model (4).

Parameter	Value	Dimension	Reference
Λ_h	140	Day^{-1}	Assumed
Λ_p	1450	Day^{-1}	[47]
β_N	2.4×10^{-11}	Day^{-1}	[31]
β_B	4×10^{-10}	Day^{-1}	Assumed
β_T	$0.064(0.083 - 0.68)/30$	Day^{-1}	[31]
β_p	0.01	Day^{-1}	[5]
μ_h	0.0141/365	Day^{-1}	[47, 48]
μ_N	4.1095×10^{-5}	Day^{-1}	Assumed
μ_p	0.083/30	Day^{-1}	[31]
α	$0.6(0.5 - 4)/7$	Day^{-1}	[49]
ω	0.132/365	Day^{-1}	[48]
σ	$10^6(640000 - 1800000)$	Day^{-1}	[49]
δ	$0.8(0.5 - 2)/365$	Day^{-1}	[29]

Since all eigenvalues are positive, the Hessian matrix is positive-definite at $\Sigma - \varepsilon^*$. Hence, $H(\Sigma - \varepsilon^*) > 0$. Next, differentiating each term in Equation (43) with respect to t gives

$$\begin{aligned} \frac{dH}{dt} = {} & \left(1 - \frac{S_h^*}{S_h}\right)\frac{dS_h}{dt} + \left(1 - \frac{I_T^*}{I_T}\right)\frac{dI_T}{dt} + \left(1 - \frac{I_N^*}{I_N}\right)\frac{dI_N}{dt} \\ & + \left(1 - \frac{S_p^*}{S_p}\right)\frac{dS_p}{dt} + \left(1 - \frac{I_p^*}{I_p}\right)\frac{dI_p}{dt} + \left(1 - \frac{P^*}{P}\right)\frac{dP}{dt} \\ & + \left(1 - \frac{E_t^*}{E}\right)\frac{dE}{dt}. \end{aligned} \tag{48}$$

Plugging system of equations of model (4) yields

$$\begin{aligned} \frac{dH}{dt} = {} & \left(1 - \frac{S_h^*}{S_h}\right)(\Lambda_h - [\beta_T P + \beta_h E + \mu_h]S_h) \\ & + \left(1 - \frac{I_t^*}{I_t}\right)(d\beta_T P S_h - [\beta_N E + \delta + \mu_h]I_t) \\ & + \left(1 - \frac{I_N^*}{I_N}\right)(\beta_N E S_h + \beta_T E I_T - [+\mu_h + \mu_N]I_N) \\ & + \left(1 - \frac{S_p^*}{S_p}\right)\left(\Lambda_P - \left(\beta_P E + \mu_p\right)S_p\right) \\ & + \left(1 - \frac{I_p^*}{I_p}\right)\left(\beta_P E S_p - \mu_p I_p\right) + \left(1 - \frac{P^*}{P}\right)(\omega I_p - \delta P) \\ & + \left(1 - \frac{E^*}{E}\right)(\sigma I_T - \alpha E). \end{aligned} \tag{49}$$

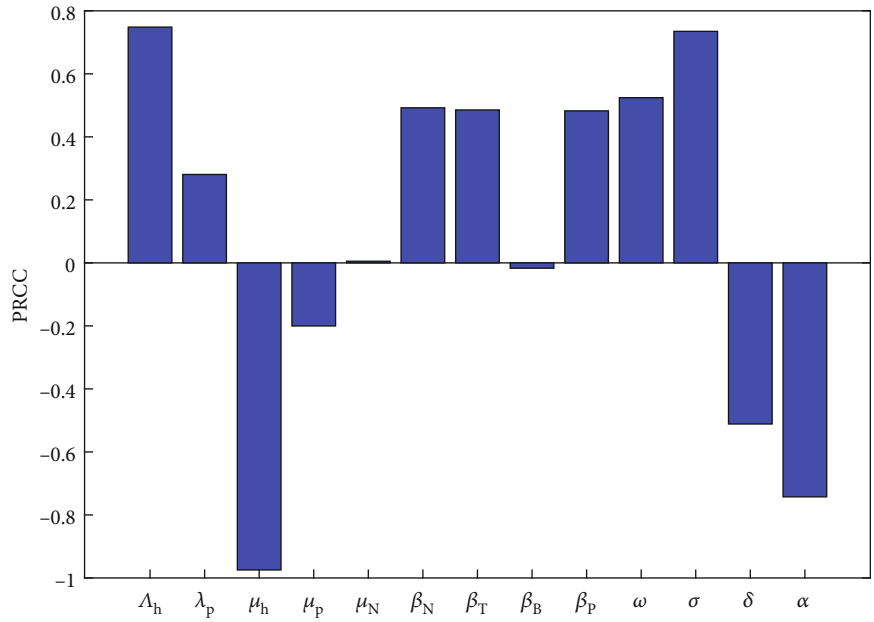

Figure 2: PRCC results for global sensitivity analysis.

Then, Equation (49) simplifies to

$$\begin{aligned}\frac{dH}{dt} &= \Lambda_h + (\beta_T P + \beta_N E + \mu_h)S_h^* + \beta_T P S_h + (\beta_h E + \mu_h)I_T^* \\ &+ \beta_N E S_h + (\beta_T P + \mu_h + \mu_N)I_N^* + \Lambda_p + \left(\beta_p E + \mu_p\right)S_p^* \\ &+ \beta_p E S_p + \mu_p I_p^* + \omega I_p + \delta P^* - (\beta_T P + \beta_N E + \mu_h)S_h \\ &- \Lambda_h \frac{S_h^*}{S_h} - (\beta_N E + \mu_h)I_T - \frac{I_T^*}{I_T}\beta_T P S_h \\ &- (\beta_T P + \mu_h + \mu_N)I_N - \frac{I_N^*}{I_N}\beta_N E S_h - \left(\beta_p E + \mu_p\right)S_p \\ &- \Lambda_p \frac{S_p^*}{S_p} - \mu_p I_p - \beta_p E S_p \frac{I_p^*}{I_p} - \delta P - \omega I_p \frac{P^*}{P} \\ &- \alpha E - \frac{E_T^*}{E}\sigma I_T.\end{aligned} \tag{50}$$

Note that dH/dt can be rewritten in the form of

$$\frac{dH}{dt} = R - Q, \tag{51}$$

where

$$\begin{aligned}R &= \Lambda_h + (\beta_T P + \beta_N E + \mu_h)S_h^* + \beta_T P S_h + (\beta_h E + \mu_h)I_T^* \\ &+ \beta_N E S_h + (\beta_T P + \mu_h + \mu_N)I_N^* + \Lambda_p + \left(\beta_p E + \mu_p\right)S_p^* \\ &+ \beta_p E S_p + \mu_p I_p^* + \omega I_p + \delta P^*,\end{aligned}$$

$$\begin{aligned}Q &= (\beta_T P + \beta_N E + \mu_h)S_h + \Lambda_h \frac{S_h^*}{S_h} + (\beta_h E + \mu_h)I_T \\ &+ \frac{I_T^*}{I_T}\beta_T P S_h + (\beta_T P + \mu_h + \mu_N)I_N + \frac{I_N^*}{I_N}\beta_N E S_h \\ &+ \left(\beta_p E + \mu_p\right)S_p + \Lambda_p \frac{S_p^*}{S_p} + \mu_p I_p + \beta_p E S_p \frac{I_p^*}{I_p} + \delta P \\ &+ \omega I_p \frac{P^*}{P} + \alpha E + \frac{E_T^*}{E}\sigma I_T.\end{aligned} \tag{52}$$

From Equation (51), it can be noted that if $R < Q$, then $dH/dt < 0$, and if $\Sigma = \Sigma^*$, then $dH/dt = 0$. From the LaSalle's invariant principle as applied in [30, 42, 43], we can ascertain that as $t \longrightarrow \infty$, and the solution of model system (4) approaches the endemic equilibrium when $\mathcal{R}_0 > 0$. Hence, the endemic equilibrium is globally asymptotically stable in the invariant set Σ if $R > Q$. □

4. Numerical Results and Discussion

We performed numerical simulations for model (4) to support the analytical results described in Section 3. We simulated sensitivity analysis, dynamics of the model system, stability of the endemic equilibrium point, and the contribution of taeniasis-infected individuals to the taeniasis and NCC coinfection burden. Using initial conditions and parameter values in Table 1, the model was simulated using an ODE solver coded in MATLAB programming language.

Most of the real data associated with taeniasis and NCC are limited in quantity and inconsistent due to underreporting and misdiagnosis [44–46]. Hence, the data used to support the findings of this study mostly are from the literature similar to this study, where unavailable data especially values of parameters were assumed for the purpose of verifying the results of the mathematical analysis of model (4).

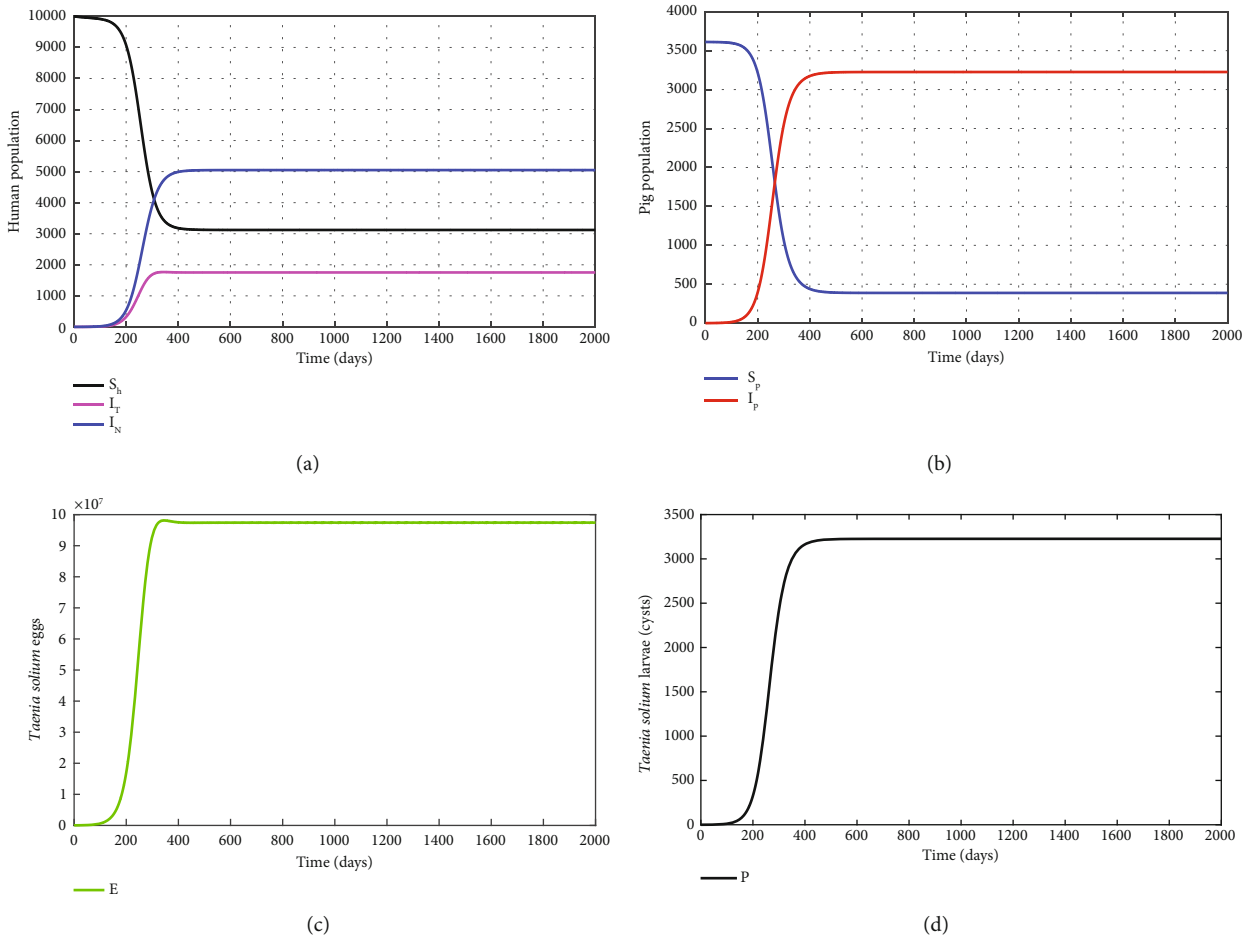

FIGURE 3: Dynamical behaviour of model (4) for (a) human population, (b) pig population, (c) concentration of *Taenia solium eggs*, and (d) concentration of cysts.

4.1. Sensitivity Analysis. First, we derived Equation (53) for the total number of potential individuals who can acquire taeniasis and NCC, denoted by P_{total}, and then computed its partial rank correlation (PRCC) [50] with parameters β_N, β_P, α, δ, and σ. Nonlinear and monotone relationship were observed for the parameters with respect to P_{total}, which is a prerequisite for performing PRCC analysis.

$$P_{\text{total}} = \int_0^T [(\beta_T P(t) + \beta_N E(t)) S_h(t)] dt. \tag{53}$$

Figure 2 shows PRCC results for $T = 2000$ days (chosen arbitrarily). The base values for parameters are given in Table 1. For each of the parameters, 1000 Latin Hypercube Samples (LHS) were generated from the interval (0.5× base value and 1.5× base value). We note that the parameters β_B, β_P, σ, and ω have significant positive correlations with P_{total}. This indicates that transmission rate of taeniasis and NCC will increase the total number of patients related to taeniasis and/or NCC.

4.2. Dynamical System of the Model. We illustrate the dynamics of taeniasis and NCC model (4) behaviour by numerically solving the model system equations. Using the initial conditions of the variables, $S_h(0) = 10000$, $I_T(0) = 1$, $I_N(0) = 1$, $S_p(0) = 3614$, $I_p(0) = 0$, $P(0) = 0$, and $E(0) = 0$.

Figure 3(a) shows that the susceptible humans decrease after contracting taeniasis and NCC. In addition, the natural death rate contributes to the decrease in these susceptible populations. The decline of susceptible individuals does not decrease to zero; it stabilizes to a nonnegative value due to the continuous recruitment rate. It is also observed that the susceptible individuals decline rapidly after the first 200 days. On the other hand, the infectious classes increase after individuals from the susceptible class acquire diseases and move to these classes. The NCC class has an additional disease-induced death rate, causing a lesser decrease. Both taeniasis and NCC classes stabilize after 400 days and 500 days, respectively.

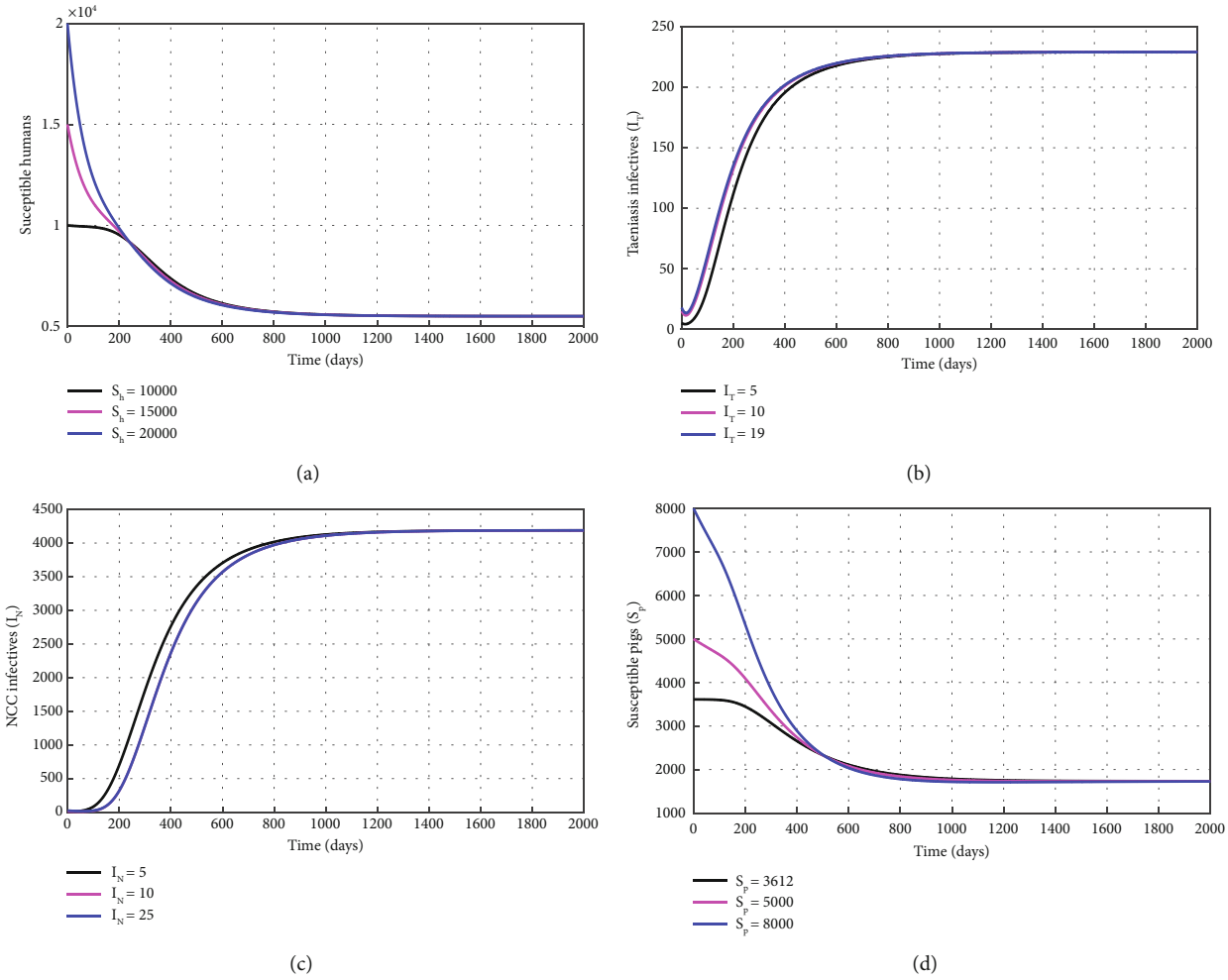

Figure 4: The global stability of the endemic equilibrium point. (a) Stability of endemic equilibrium for susceptible humans. (b) Stability of endemic equilibrium for infected humans with taeniasis. (c) Stability of endemic equilibrium for infected humans with both taeniasis and NCC. (d) Stability of endemic equilibrium for cysts-infected pigs.

In Figure 3(b), we observe that susceptible pigs decrease after ingestion of *Taenia solium* eggs from the contaminated environment, get infected, and move to the infectious class. The decrease also contributed to the natural death rate. It is noted that after the first 250 days, susceptible pigs decrease rapidly but stabilize after the 650 days. However, the infectious class increases after 250 days and stabilizes after the first 800 days.

Figures 3(c) and 3(b) illustrate the dynamics of *Taenia solium* eggs concentration in the contaminated environment and the concentration of *Taenia solium* larvae cysts in the contaminated pork products, respectively. We observe from the graphs that the *Taenia solium* eggs increase after the first 150 days, stabilize to a nonnegative number, and stay in that state indefinitely. This increase is a result of an increase in the number of infected humans with taeniasis and the shedding rate of the eggs in the environment. In addition, Figure 3(d) demonstrates the dynamics of cysts, whereby an increase in the rate of consuming cysts from the infected pork products, result in an increase in the *Taenia solium* eggs. However, the removal rate of the *Taenia solium* eggs and cysts lead to a decrease in their concentrations.

4.3. Stability of the Endemic Equilibrium Point. Figure 4 indicates that the endemic equilibrium point of model (4) is globally stable, and the system comes to an equilibrium point from any possible initial conditions. For the purpose of demonstration, we show endemic simulation for human and susceptible pig populations.

4.4. Visualization of the Role Played by Taeniasis Infectives in NCC Dynamics. Numerical simulations in Figure 5 show the effect of varying the infectious coefficient of taeniasis on the taeniasis and the coinfected human populations. As the value of β_T is increased, Figure 5 affirms that the taeniasis infectives, coinfected human populations, and the infected pigs also increase. This is an obvious indication that the role taeniasis infectives play in the dynamics of taeniasis and NCC transmission should not be disregarded.

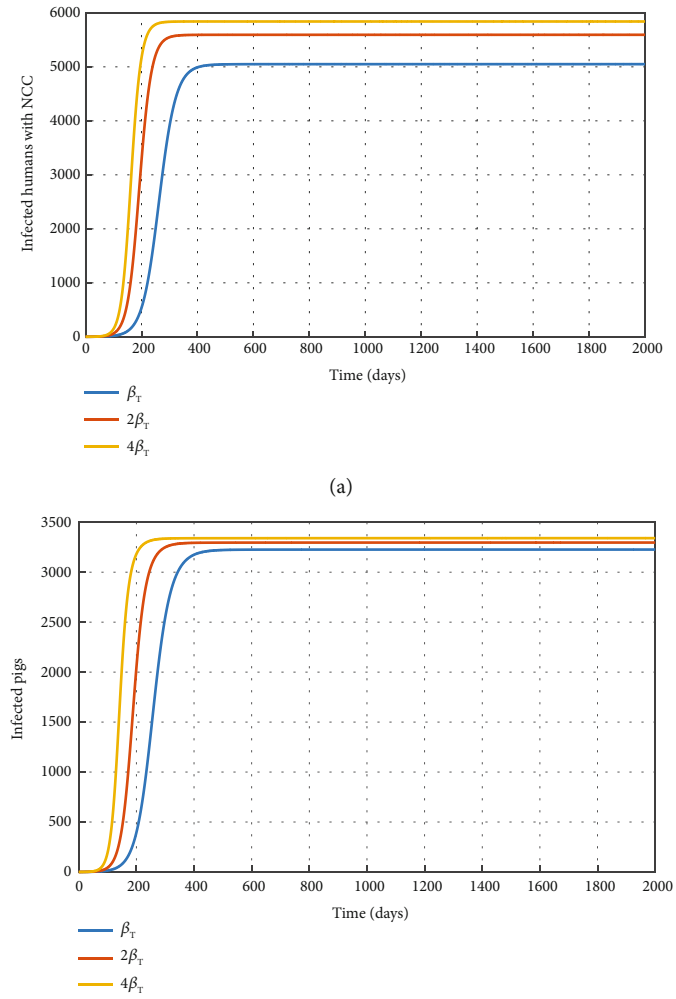

Figure 5: Effect of taeniasis infectives on codynamics of taeniasis and NCC.

5. Conclusion

It was pointed out that NCC is a serious public health problem in *Taenia solium* endemic areas. Elimination of Taenia solium, the causative agent of the disease, remains a key intervention method for controlling NCC. Contracting the contaminated environment with *Taenia Solium* and the infected pork products are driving factors of taeniasis and NCC in the community. As such, in this work, the taeniasis and NCC codynamics model is formulated and analyzed. The basic properties of the model are shown. We discussed numerous qualitative properties of the model such as the positivity of the solution set, invariant region, equilibria points, basic reproductive number, and stability of nature of equilibrium points. We established that disease-free equilibrium is globally asymptotically stable when the basic reproduction numbers are less than unity. By using suitable Lyapunov functions, the equilibrium E_1 is globally asymptotically stable whenever $\mathcal{R}_0 > 1$.

The sensitivity analysis of the formulated Equation (53) for infected humans shows that most of the parameters and particularly easily addressable parameters have a dominant role in disease transmission. Numerical simulations show that the increased infectivity of taeniasis infectives increases the number of NCC infections in humans. Further, simulations dictate that reducing the rate of consuming improperly cooked or raw pork meat and the ingestion of *Taenia solium* eggs through good hygiene and sanitation is of great importance towards reducing the burden of NCC infection and its close association with taeniasis.

Further investigation of the influence of variations in the model's parameters on the taeniasis and NCC was carried out through numerical simulations. In view of the findings from this study, it was recommended that health management decision-makers should implement policies that would make more people become medically hygienic and practice proper cooking of pork meat so that the spread of the disease can stem as the community is gradually driven towards a taeniasis/NCC free.

In the future, we intend to extend this study by including the optimal control and study the impact of public health education and vaccination of pig swarms in controlling these preventable diseases; the model dynamical behaviour will be considered as a discrete time.

Data Availability

The data for parameters used in the model simulation is obtained from the literature, and the references are cited in the manuscript.

Conflicts of Interest

The authors declare that there is no conflict of interest regarding the publication of this article.

Authors' Contributions

Gideon Eustace Rwabona was responsible for the conceptualization, methodology, visualization, software, writing—original draft, and writing—review and editing. Verdiana Grace Masanja was responsible for the conceptualization, supervision, review, and editing. Sayoki Mfinanga was responsible for the conceptualization, supervision, review, and editing. Abdoelnaser Degoot was responsible for the conceptualization, supervision, review, and editing. Silas Mirau was responsible for the supervision, review, and editing.

Acknowledgments

The authors are grateful to Mbeya University of Science and Technology, The Nelson Mandela African Institution of Science and Technology, and The African Institute for Mathematical Sciences for providing extreme workspaces and resources. Also, appreciation goes to Dr. Diana Nicodemas for her advice and encouragement.

References

[1] Z. S. Pawlowski, "Role of chemotherapy of taeniasis in prevention of neurocysticercosis," *Parasitology International*, vol. 55, pp. S105–S109, 2006.

[2] D. Stelzle, V. Schmidt, L. Keller et al., "Characteristics of people with epilepsy and neurocysticercosis in three eastern African countries–a pooled analysis," *PLOS Neglected Tropical Diseases*, vol. 16, no. 11, article e0010870, 2022.

[3] O. H. Del Brutto, "Neurocysticercosis: a review," *The Scientific World Journal*, vol. 2012, Article ID 159821, 8 pages, 2012.

[4] M. Verastegui and A. Gonzalez, "Experimental infection model for Taenia solium cysticercosis in swine. Cysticercosis Working Group in Peru," *Veterinary Parasitology*, vol. 94, no. 1-2, pp. 33–44, 2000.

[5] N. C. Kyvsgaard, M. V. Johansen, and H. Carabin, "Simulating transmission and control of Taenia solium infections using a reed-frost stochastic model," *International Journal for Parasitology*, vol. 37, no. 5, pp. 547–558, 2007.

[6] H. Carabin, P. C. Ndimubanzi, C. M. Budke et al., "Clinical manifestations associated with neurocysticercosis: a systematic review," *PLoS Neglected Tropical Diseases*, vol. 5, no. 5, article e1152, 2011.

[7] W. Liu and D. Liu, "Molecular control of Taenia solium cysticercosis," in *Molecular Food Microbiology*, pp. 479–488, CRC Press, 2021.

[8] World Health Organization, *Who Guidelines on Management of Taenia solium Neurocysticercosis*, WHO, 2021.

[9] D. G. D. Maes, J. Dewulf, C. Pineiro, S. Edwards, and I. Kyriazakis, "A critical reflection on intensive pork production with an emphasis on animal health and welfare," *Journal of Animal Science*, vol. 98, Supplement_1, pp. S15–S26, 2020.

[10] L. A. Soto, L. A. Parker, M. J. Irisarri-Gutierrez et al., "Evidence for transmission of Taenia solium taeniasis/cysticercosis in a rural area of northern *Rwanda*," *Science*, vol. 8, article 645076, 2021.

[11] World Health Organization, "The world health organization 2030 goals for Taenia solium: Insights and perspectives from transmission dynamics modelling: Cystiteam group for epidemiology and modelling of Taenia solium taeniasis/cysticercosis," *Gates Open Research*, vol. 3, 2019.

[12] C. Butala, T. M. Brook, A. OMajekodunmi, and S. C. Welburn, "Neurocysticercosis: current perspectives on diagnosis and management," *Frontiers in Veterinary Science*, vol. 8, article 615703, 2021.

[13] G. Bonnet, F. Pizzitutti, E. A. Gonzales-Gustavson et al., "Cystihuman: a model of human neurocysticercosis," *PLoS Computational Biology*, vol. 18, no. 5, article e1010118, 2022.

[14] S. Gabriel, D. Pierre, and K. E. Mwape, "Control of Taenia solium taeniasis/cysticercosis: the best way forward for sub-Saharan Africa?," *Acta Tropica*, vol. 165, pp. 252–260, 2017.

[15] C. Nyangi, D. Stelzle, E. M. Mkupasi et al., "Knowledge, attitudes and practices related to Taenia solium cysticercosis and taeniasis in Tanzania," *BMC Infectious Diseases*, vol. 22, no. 1, p. 534, 2022.

[16] V. Schmidt, M.-C. O'Hara, B. Ngowi et al., "Taenia solium cysticercosis and taeniasis in urban settings: Epidemiological evidence from a health-center based study among people with epilepsy in Dar es Salaam, Tanzania," *PLoS Neglected Tropical Diseases*, vol. 13, no. 12, article e0007751, 2019.

[17] H. A. Ngowi, A. SylviaWinkler, U. C. Braae et al., "Taenia solium taeniosis and cysticercosis literature in Tanzania provides research evidence justification for control: a systematic scoping review," *PLoS One*, vol. 14, no. 6, article e0217420, 2019.

[18] B. J. Mwang'onde, M. J. Chacha, and G. Nkwengulila, "The status and health burden of neurocysticercosis in Mbulu district, northern Tanzania," *BMC Research Notes*, vol. 11, no. 1, pp. 1–5, 2018.

[19] L. F. Owolabi, B. Adamu, A. M. Jibo, S. D. Owolabi, A. I. Imam, and I. D. Alhaji, "Neurocysticercosis in people with epilepsy in sub Saharan Africa: a systematic review and meta-analysis of the prevalence and strength of association," *Seizure*, vol. 76, pp. 1–11, 2020.

[20] B. Fatima, M. Yavuz, M. u. Rahman, and F. S. al-Duais, "Modeling the epidemic trend of middle eastern respiratory syndrome coronavirus with optimal control," *Mathematical Biosciences and Engineering*, vol. 20, no. 7, pp. 11847–11874, 2023.

[21] M. U. Rahman, G. Alhawael, and Y. Karaca, "Multicompartmental analysis of middle eastern respiratory syndrome coronavirus model under fractional operator with next-generation matrix methods," *Fractals*, vol. 31, no. 10, pp. 1–20, 2023.

[22] B. Fatima, M. Yavuz, M. Rahman, A. Althobaiti, and S. Althobaiti, "Predictive modeling and control strategies for the transmission of Middle East respiratory syndrome coronavirus," *Mathematical and Computational Applications*, vol. 28, no. 5, p. 98, 2023.

[23] B. Li, Z. Eskandari, and Z. Avazzadeh, "Dynamical behaviors of an sir epidemic model with discrete time," *Fractal and Fractional*, vol. 6, no. 11, p. 659, 2022.

[24] M. R. TariqMahmood, M. Arfan, S.-I. Kayani, and M. Sun, "Mathematical study of algae as a bio-fertilizer using fractal–fractional dynamic model," *Mathematics and Computers in Simulation*, vol. 203, pp. 207–222, 2023.

[25] D. Li, "Development and validation of a mathematical model for growth of pathogens in cut melons," *Journal of Food Protection*, vol. 76, no. 6, pp. 953–958, 2013.

[26] S. Osman, O. D. Makinde, and D. M. Theuri, "Mathematical modelling of listeriosis epidemics in animal and human population with optimal control," *Tamkang Journal of Mathematics*, vol. 51, no. 4, pp. 261–287, 2020.

[27] G.-Q. Sun, J.-H. Xie, S.-H. Huang, Z. Jin, M.-T. Li, and L. Liu, "Transmission dynamics of cholera: mathematical modeling and control strategies," *Communications in Nonlinear Science and Numerical Simulation*, vol. 45, pp. 235–244, 2017.

[28] U. C. Braae, B. Devleesschauwer, S. Gabriel et al., "Cystisim–an agent-based model for Taenia solium transmission and control," *PLoS Neglected Tropical Diseases*, vol. 10, no. 12, article e0005184, 2016.

[29] M. V. Jose, J. R. Bobadilla, N. Y. Sanchez-Torres, and J. P. Laclette, "Mathematical model of the life cycle of Taenia-cysticercosis: transmission dynamics and chemotherapy (part 1)," *Theoretical Biology and Medical Modelling*, vol. 15, no. 1, pp. 1–19, 2018.

[30] J. A. Mwasunda, J. I. Irunde, D. Kajunguri, and D. Kuznetsov, "Modeling and analysis of taeniasis and cysticercosis transmission dynamics in humans, pigs and cattle," *Advances in Difference Equations*, vol. 2021, no. 1, 23 pages, 2021.

[31] P. Winskill, W. E. Harrison, M. D. French, M. A. Dixon, B. Abela-Ridder, and M.-G. Basanez, "Assessing the impact of intervention strategies against Taenia solium cysticercosis using the epicyst transmission model," *Parasites & Vectors*, vol. 10, no. 1, p. 73, 2017.

[32] M. A. Dixon, U. C. Braae, P. Winskill et al., "Modelling for Taenia solium control strategies beyond 2020," *Bulletin of the World Health Organization*, vol. 98, no. 3, pp. 198–205, 2020.

[33] O. Diekmann, J. A. P. Heesterbeek, and J. A. J. Metz, "On the definition and the computation of the basic reproduction ratio r 0 in models for infectious diseases in heterogeneous populations," *Journal of Mathematical Biology*, vol. 28, no. 4, pp. 365–382, 1990.

[34] P. Van den Driessche and J. Watmough, "Reproduction numbers and sub-threshold endemic equilibria for compartmental models of disease transmission," *Mathematical Biosciences*, vol. 180, no. 1-2, pp. 29–48, 2002.

[35] M. Jane, "Perspectives on the basic reproductive ratio," *Journal of the Royal Society Interface*, vol. 2, no. 4, pp. 281–293, 2005.

[36] F. Nyabadza, Z. Mukandavire, and S. D. Hove-Musekwa, "Modelling the HIV/AIDS epidemic trends in South Africa: insights from a simple mathematical model," *Nonlinear Analysis: Real World Applications*, vol. 12, no. 4, pp. 2091–2104, 2011.

[37] J. P. LaSalle, "Stability theory and invariance principles," in *Dynamical Systems*, pp. 211–222, Elsevier, 1976.

[38] S. U. Pillai, T. Suel, and S. Cha, "The Perron-Frobenius theorem: some of its applications," *IEEE Signal Processing Magazine*, vol. 22, no. 2, pp. 62–75, 2005.

[39] A. Mhlanga, "Assessing the impact of optimal health education programs on the control of zoonotic diseases," *Computational and Mathematical Methods in Medicine*, vol. 2020, Article ID 6584323, 15 pages, 2020.

[40] R.-S. Yuan, B. Y. Yi-AnMa, and P. Ao, "Lyapunov function as potential function: a dynamical equivalence," *Chinese Physics B*, vol. 23, no. 1, article 010505, 2013.

[41] Y. Wei, J. Cao, Y. Chen, and Y. Wei, "The proof of Lyapunov asymptotic stability theorems for Caputo fractional order systems," *Applied Mathematics Letters*, vol. 129, article 107961, 2022.

[42] O. Ofosuhene, "Using stochastic dynamic modelling to estimate the sensitivity of current and alternative surveillance program of Salmonella in conventional broiler production," *Scientific Reports*, vol. 10, no. 1, article 19441, 2020.

[43] H. Damak and M. A. Hammami, "Stabilization and practical asymptotic stability of abstract differential equations," *Numerical Functional Analysis and Optimization*, vol. 37, no. 10, pp. 1235–1247, 2016.

[44] G. Zulu, D. Stelzle, K. E. Mwape et al., "The epidemiology of human Taenia solium infections: a systematic review of the distribution in eastern and southern Africa," *PLoS Neglected Tropical Diseases*, vol. 17, no. 3, article e0011042, 2023.

[45] P. R. Torgerson and P. Craig, "Investigating the Burden of Parasitic Zoonotic Diseases," in *The control of neglected zoonotic diseases: community-based interventions for prevention and control*, WHO Headquarters, Geneva, Switzerland, 2010.

[46] World Health Organization, *The control of neglected zoonotic diseases: community based interventions for nzds prevention and control: report of the third conference organized with iconz, dfidriu, sos, eu, tdr and fao with the participation of ilri and oie: 23-24 November 2010*, Technical report, Who heaquarters, Geneva, Switzerland, 2011.

[47] J. Mwasunda, *Modelling the Transmission Dynamics and Control of Taeniasis and Cysticercosis in Humans, Pigs and Cattle, [Ph.D. thesis]*, NM-AIST, 2022.

[48] J. I. Irunde and F. B. Luhanda, "Taenia solium taeniasis and cysticercosis: extinction or outbreak," *Animal Diseases*, vol. 3, no. 1, 2023.

[49] I. WPray, W. Wakeland, W. Pan et al., "Understanding transmission and control of the pork tapeworm with cystiagent: a spatially explicit agent-based model," *Parasites & Vectors*, vol. 13, no. 1, 2020.

[50] S. Marino, I. B. Hogue, C. J. Ray, and D. E. Kirschner, "A methodology for performing global uncertainty and sensitivity analysis in systems biology," *Journal of Theoretical Biology*, vol. 254, no. 1, pp. 178–196, 2008.